Acta Scientiarum
http://periodicos.uem.br/ojs
ISSN on-line: 1807-8664
https://doi.org/10.4025/actascitechnol.v48i1.74146

Application of Artificial Neural Networks (ANN) for modeling Personalized Ventilation Systems (PVS) using CFD data

Marlon Breno Amora Ribeiro[1*], Álvaro Messias Bigonha Tibiriçá[1], André Luiz de Freitas Coelho[2], Júlio César Costa Campos[1] and Henrique Márcio Pereira Rosa[1]

[1]Departamento de Engenharia de Produção e Mecânica, Universidade Federal de Viçosa, Avenida PH Rolfs, s/n, 36570-900, Viçosa, Minas Gerais, Brazil. [2]Departamento de Engenharia Agrícola, Universidade Federal de Viçosa, Viçosa, Minas Gerais, Brazil. *Autor for correspondente. E-mail: marlonbrenoribeiro@outlook.com

ABSTRACT. This study investigates the application of Artificial Neural Networks (ANNs) for modeling Personalized Ventilation Systems (PVS) using data from Computational Fluid Dynamics (CFD) simulations. In recent years, machine-learning techniques like ANNs have been increasingly used to accelerate CFD analysis and improve the accuracy of temperature and airflow velocity predictions in indoor environments. The methodology involved conducting twelve CFD simulations in a three-dimensional space, followed by data filtering and normalization to train and test the neural network. The room was composed of two individuals, positioned side by side, both seated and receiving air from a ceiling supply system. Both individuals were modeled to maintain a constant surface temperature while also transferring heat to the environment. The quality of the results were analyzed by comparing the neural network outputs with data that had been omitted from the network. The results demonstrated the effectiveness of the model, with average errors ranging from 1% to 3% and maximum errors between 6% and 15%. This approach significantly reduces the computational time required for traditional CFD simulations while maintaining high accuracy, offering promising prospects for optimizing PVS performance in various indoor settings. The use of machine learning makes the analysis and design of personalized ventilation systems faster and more efficient, with practical applications in offices, classrooms, and residential spaces.

Keywords: Machine Learning; Computational Fluid Dynamics; Air Conditioning; Predictive model; Indoor airflow.

Received on October 10, 2024.
Accepted on February 03, 2025.

Introduction

A personalized ventilation system is a ventilation system custom designed to meet the specific needs of an individual or a particular space, as opposed to conventional ventilation, which treats with a general area. It allows for the control and adjustment of ventilation conditions, such as airflow rate, temperature, and air quality, based on the preferences and requirements of a particular person. These systems are often used in environments such as offices, classrooms, and residences to enhance the thermal comfort, air quality, and energy efficiency by providing a more personalized and effective ventilation experience.

The efficiency of ventilation systems plays a key role in ensuring the comfort and safety of occupants in indoor environments. Customizing these ventilation systems is crucial to cater to individual needs, considering factors like temperature distribution and air velocity in enclosed spaces. However, conducting Computational Fluid Dynamics (CFD) simulations to design personalized ventilation systems is a complex task that often consumes a considerable amount of time.

In their work, Katramiz et al. (2021) initially assessed the evaluation of contaminants expelled by a single user in a closed room. Subsequently, the same authors, Katramiz et al. (2021), introduced a system with air supply from the desk and evaluated the dispersion of contaminants generated by users to each other. The progression from a single-user analysis to one involving two users is evident in a lot of places. However, this progression results in an increase in the time required to generate results.

Rissetto et al. (2021) also explores the use of personalized ventilation systems. In this study, an evaluation of six different jet inflow angles are conducted for an individual positioned in six different locations. This is further analyzed by Xu et al. (2020), who investigates the flow effects of personalized ventilation systems. The study assesses the efficiency of a PV system at varying angles originating from a desk inflow. The application of machine learning could potentially enhance processing time and facilitate the study of new cases in both research endeavors.

The demand for solutions that optimize analysis time has surged with the growing complexity of personalized ventilation projects. Xu et al. (2021) delve into the analysis of modeling strategies, with the primary goal of enhancing both precision and processing efficiency within confined environments. Their approach involves the utilization of tetrahedra, hexahedra, and polyhedra as mesh elements to fine-tuning the cost-effectiveness of their simulations. The article underscores the manifold advantages associated with the application of such modeling strategies but also highlights the substantial demand on computational memory resources.

In this context, the application of neural networks, a machine learning technique, has shown as a great promise. Neural networks can be employed to expedite the analysis of CFD simulations, enabling a quicker and more efficient assessment of ventilation conditions. Jing et al. (2023) have contributed to the field by introducing a new physics-guided neural network framework for rapid full-field temperature prediction in indoor environments. Their approach, comprising surrogate, discrepancy, and recovery models, effectively bridges the gap between numerical simulations and real-world applications, improving full-field temperature predictions for indoor spaces, even when dealing with limited measured data.

Tian et al. (2021) investigated ventilation methods like stratum and displacement ventilation for efficient indoor environments and energy savings. It highlights challenges in managing conditions across different heights within a room and uses the back-propagation (BP) model in artificial neural networks to predict energy performance, thermal comfort, and indoor air quality. Through CFD cases, the study shows the BP model's superior accuracy compared to linear regression, especially in indoor environment prediction. Interestingly, air velocity information was redundant for cooling predictions but improved thermal comfort during heating. The addition of a genetic algorithm slightly enhanced indoor air quality prediction during heating. Validation with experimental data confirmed the robustness of developed ANN models across various scenarios in both ventilation methods.

Jing et al. (2023) proposed a method based on neural networks and physics to rapidly predict full-field temperature in indoor environments. The model comprised three main components: a neural network-based surrogate model, a discrepancy model using transfer learning, and a recovery model integrating both. This approach proved effective in providing accurate predictions with a limited number of measured data, reducing the gap between numerical simulation and the real world.

Li et al. (2022) introduced a Computational Fluid Dynamics (CFD)-based Back Propagation Neural Network (BPNN) combined with a Particle Swarm Optimizer (PSO) algorithm. The BPNN-PSO method accurately predicts and optimizes IAQ (Indoor Air Quality) with minimal CFD runs. Compared to other methods, BPNN-PSO reduces indoor air pollutant concentration by up to 6.44% and computational costs by 23.53%. Leveraging CFD ensures accurate information acquisition, enabling rapid prediction of indoor environmental conditions. The BPNN-PSO algorithm holds promise for effective and intelligent indoor ventilation strategies.

Zhou and Ooka (2021c) investigate the synergy between energy efficiency and indoor thermal comfort in building design, emphasizing the need to integrate building energy performance and indoor environmental quality considerations. They employ coupled simulations involving building energy simulation (BES) and computational fluid dynamics (CFD) to provide complementary insights. However, CFD's computational cost hinders its widespread use, prompting exploration into the potential of neural networks (NNs) as a promising CFD alternative. Their research aims to verify NN's feasibility for predicting indoor airflow in a three-dimensional space. The NN, using boundary conditions as input, produces velocity and temperature distributions. Comparative analysis against CFD simulations reveals NN's accuracy, with relative errors below 12%, and significant time savings of 80%.

Kim and Park (2023) present a new approach for predicting thermodynamic parameters in indoor environments using artificial neural networks (ANN). They employ two independently trained ANN models, with the second model receiving the velocity distribution prediction from the first as an additional input to predict pressure and temperature distributions. Validation using computational fluid dynamics (CFD) data with 100 case scenarios demonstrates the model's improved performance, surpassing existing ANN models and offering a viable solution for indoor airflow prediction. These innovative approaches hold the potential to revolutionize the study and application of personalized ventilation systems.

Personalized ventilation systems with ANNs remain an underexplored area in published literature, lacking comprehensive studies and analyses. Introducing artificial neural networks (ANNs) in Computational Fluid Dynamics (CFD) research for personalized ventilation systems holds significant promise in enhancing the study's speed and efficiency. Leveraging ANNs can expedite simulations, potentially accelerating the design and evaluation processes for these personalized ventilation systems.

Materials and methods

The methodology has been structured into five steps. In the first step, Data and CFD simulation, CFD simulations are conducted to model an environment with a customized air conditioning system. The second step, Filtering and Standardization, involves standardizing and normalizing data for uniform analysis. Assembly of the network outlines the implementation of neural networks to predict temperature and velocity. Subsequently, Processing Time introduces methods to assess the processing time between CFD and neural networks. Lastly, Results Analysis and Comparison presents the equations used to evaluate the accuracy of the developed models compared to other studies.

Data and CFD simulation

The initial results of this study were obtained through CFD simulations, using Ansys Inc. software. The investigated environment is a room with dimensions of 3 meters in length, 3 meters in width, and 3 meters in height, with the air supply system coming from the ceiling aimed at providing thermal comfort to two occupants. Furthermore, the room has four strategically positioned openings in the upper corners, as illustrated in Figure 1, to ensure an effective distribution of air in the space.

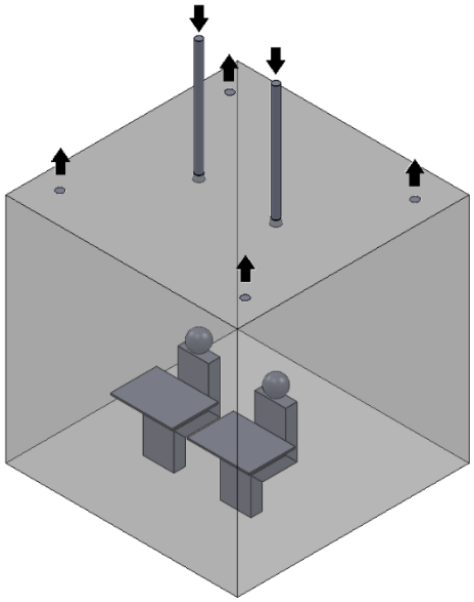

Figure 1. Representation of the model room for CFD simulations.

The initial mesh for the simulations consisted of tetrahedral, employing a cone-based approach around the users using spheres of influence. The user's surface, as well as the walls and ceiling of the room, were prescribed at a fixed temperature, utilizing heat transfer patterns for software-defined surfaces. However, temperatures were not specified for the floor in front of the user and the ground. The boundary conditions applied to all simulations are detailed in Table 1.

Table 1. Distribution of evaluated temperatures and velocities.

Boundary conditions	
Wall Temperature	27°C
User Temperature	34°C

The jet development was achieved by extending the inflow cylinders one meter above the ceiling, which remained thermally isolated from the fluid. The SST turbulence model was employed, and refinement was carried out using inflations near the surfaces. An inflow device was introduced in the air inlet region to focus the air distribution towards the user.

The data was classified based on temperature and inflow velocity information. Among the available data, nine sets were specifically isolated for the neural network learning process, while another three were exclusively reserved for the model testing and evaluation step, as highlighted in Table 2. Simulations marked

with an asterisk (*) were used to improve and validate the final results, while the remaining simulations were employed for the purpose of training the neural network.

Table 2. Distribution of inlet temperatures and velocities.

		Velocity (m s^{-1})				
		1	2	3	4	5
Temperature (°C)	15	T15V1	T15V2*	T15V3	T15V4	T15V5
	18	T18V1	T18V2	T18V3	T18V4	T18V5*
	20	T20V1	T20V2	T20V3*	T20V4	T20V5

Filtering and Standardization

To ensure a standardized and uniform analysis, a Python script was developed to resize the results into a new grid following a specific set of steps (Figure 2a):

i. Enclosure of the Room in a Larger Prism: The initial room was encapsulated within a prism of larger dimensions. (Figure 2b)

ii. Division of the Prism into Equal Cubes: The prism was subdivided into a predefined number of identical cubes, each with its relative coordinates. (Figure 2c)

iii. Mapping Room Points to Cubes: Each point in the original room was mapped and assigned to its respective cube within the new prism.

iv.Conversion of Temperature to Celsius: Temperatures were converted to Celsius units to ensure uniformity.

v. Removal of Empty or Null-Valued Cubes: Any cubes that did not contain points or had null temperatures and velocities were excluded.

vi.Calculation of Average Temperature and Speed per Cube: The temperature and velocity of each cube was calculated based on the arithmetic average of all the points within it (Figure 2d).

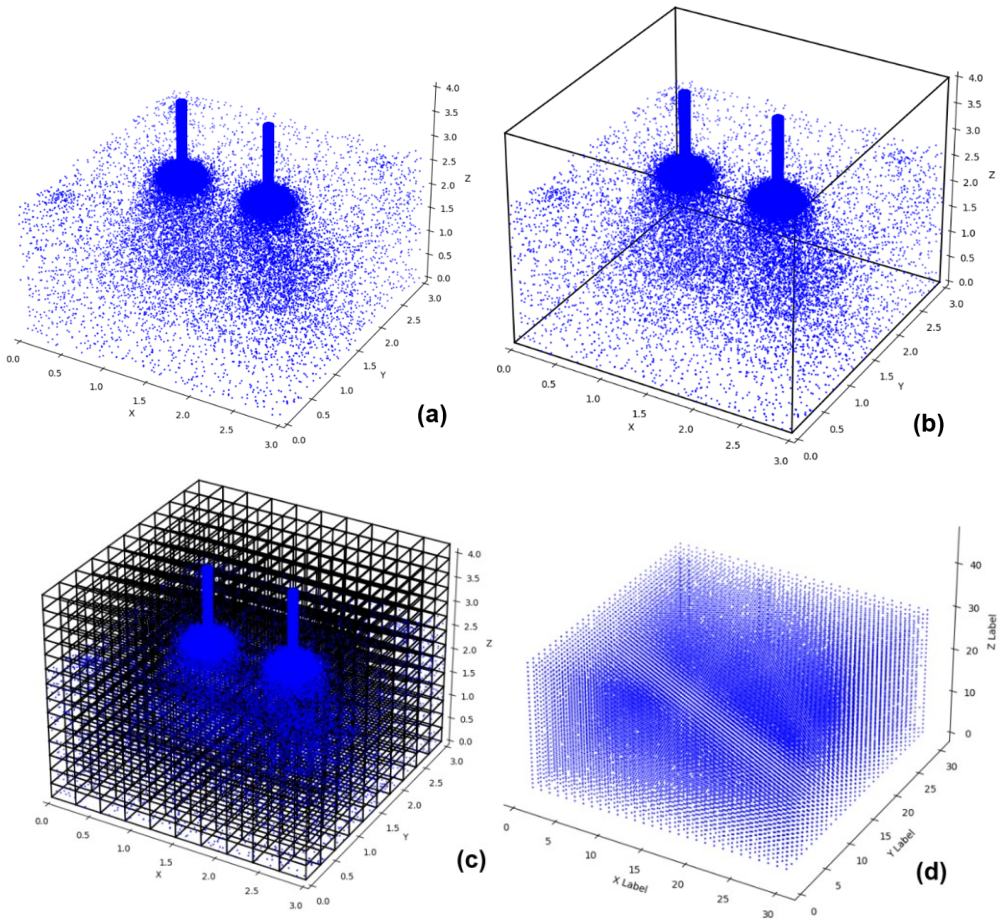

Figure 2. Mesh structuring process.

The context of the room under study, an initial division into 40,500 cubes was established, each with dimensions of 30 mm. However, after the execution of the detailed process mentioned earlier, which involved the removal of unnecessary cubes. The number was optimized to 26,462 cubes, providing a representation of the environment in a points cloud as depicted in Figure 2. Furthermore, it is important to highlight that the normalization adopted for the temperature and velocity variables was the min-max technique, resulting in normalized data ranging from 0 to 1. This ensured that the information was on a uniform scale and facilitated the analysis and interpretation of the results.

Assembly of the network

The implementation of the neural network was carried out using the Python programming language and the TensorFlow library. The architecture of the network was designed with two essential inputs, represented by inlet temperature and velocity as input variables. The neural network's output was configured to correspond to each of the 26,462 data grid cubes, resulting in a total of 26,462 individual outputs. To meet the specific analysis requirements, two distinct neural networks were developed. One of them was designed for temperature prediction, as illustrated in Figure 3, while the other aimed to predict velocity, as represented in Figure 4.

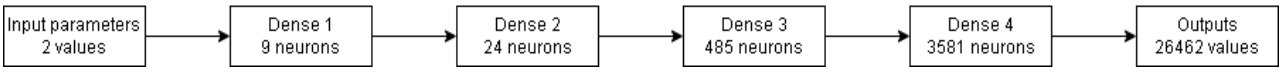

Figure 3. Network structure for temperature prediction.

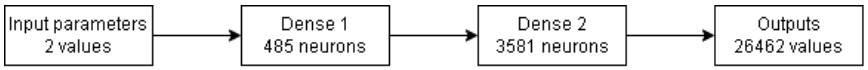

Figure 4. Network structure for velocity prediction.

The hyperparameters (the adjustable settings in a machine learning algorithm that influence its performance and must be defined before the model training) for configuring the neural network were selected through a Bayesian optimization process. To perform this optimization, the Optuna library was used, providing an effective method for finding the optimal values of hyperparameters. The hyperparameters that underwent the variation and optimization process included the learning rate, batch size and the number of epochs for each neural network as showed in Table 3.

Table 3. ANN hyperparameters.

Parameter	ANN
Learning rate	0,001
Batch size	2
Epochs	10000
Optimizer	Adam
Loss function	MSE
Activation function	Linear and ReLu

Processing Time

A fundamental aspect of our approach involves a comprehensive comparison between the neural network's predictions and the data obtained from CFD simulations. This comparative analysis will enable us to assess the accuracy and reliability of the neural network's results in predicting ventilation conditions. This assessment will be followed by a comparison with the average processing time for a simulation. Additionally, we will assess the time it takes for the machine to predict the required data for the room from random input data. The computer's technical specifications are demostrade below:

- Processor: AMD Ryzen™ 7 5700G
- RAM: 32GB DDR4 at 3200MHz
- Graphics: Radeon™ Graphics 2000MHz

The processing time denotes the average duration required for CFD simulation processing, while learning time represents the duration necessary for the machine to assimilate patterns within these simulations. Result time indicates the period post-learning, enabling the network to promptly deliver results for any input. Notably, in Table 4, an impressive 99% reduction in CFD processing time is observed upon employing an

artificial neural network to learning the pattern. Furthermore, post-training, the network exhibits the capability to instantly furnish results for any input (Temperature and Velocity)

Table 4. Distribution of evaluated temperatures and velocities.

Process	Time
Processing Time (CFD)	01:51:12
Learning Time (NNs)	08:32:34
Result Time	00:00:13

Results analysis and comparison

In the process of evaluating the results, two crucial aspects were taken into account: comprehensive analysis and a focus on critical errors (The absolute difference between the CFD result and the ANN for the same point), defined as the worst 5% of identified errors. To quantify the effectiveness of the developed models, two essential metrics were employed: RMSE (Equation 1), which provides a measure of overall accuracy of the results, and r^2 (Equation 2), which assesses the model's explanatory capability. Additionally, the average error and maximum error were considered, providing a comprehensive view of the quality of predictions in comparison to the actual data.

$$\text{RMSE} = \sqrt{\sum_i^n \frac{(\hat{y}-y_i)^2}{n}} \quad (1)$$

$$r^2 = 1 - \frac{\sum_i^n (\hat{y}_i - y_i)^2}{\sum_i^n (y_i - \bar{y}_i)^2} \quad (2)$$

where $\hat{y}$ is the real value, [°C or m s^{-1}], y_i is the predicted value, [°C or m s^{-1}], $\bar{y}$ is the average of the real values, [°C or m s^{-1}], and n is the number of points, [no unit].

The results obtained in this study were subjected to a comparative analysis with the final results of articles published in highly relevant academic journals. For this comparison, five papers were selected: Zhou and Ooka (2021a), Kim and Park (2023), Saiyad et al. (2021), Zhou and Ooka (2021b) and Zhou and Ooka (2021c). The assessment covered various areas, including regions of interest related to the individual and the development of the air jet.

Additionally, as part of the study, a cylinder model was created that encompassed the individual's contour, with dimensions as illustrated in Figure 5. For the evaluation of the air jet, the same criteria and metrics used to assess the conditions around the individual were applied, as seen in Figure 5. This included the use of metrics in cylinder, such as RMSE, r^2, average error and maximum error.

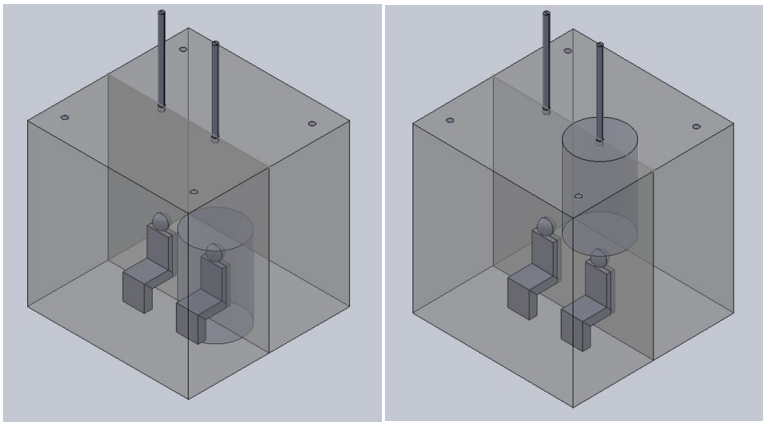

Figure 5. Region of analysis within the individual's envelope and air jet development analysis region.

Results and discussion

The results section explores five points. Results Analysis of middle plane room visually compares the temperature and velocity distributions between the network and CFD simulations in the room, emphasizing patterns recognition. Critical Errors highlights acceptable variations in temperature and velocity without discernible systematic errors. Error distribution analysis shows consistent temperature behavior and acceptable velocity variations. Comparative Analysis demonstrates consistently lower average errors and underscores the importance of a holistic assessment, comparing results of articles. Lastly, the Comprehensive Room Analysis presents detailed error insights across different room contexts, emphasizing the model's precision in various spatial scenarios.

Results Analysis of middle plane room

The air inflow in this figure is coming from the ceiling at a velocity of 2 m s^{-1} and a temperature of 15ºC. Slight variations in room temperature can be observed; however, the similarity between the temperature contours observed in the room is clear. Regions where temperature variation pockets occur are seen in both cases, demonstrating how the network was able to project patterns of regions with high temperature gradients. When comparing velocity, there is no clear difference overall in the room. Unlike the temperature-related results, both a low absolute variation and a similar velocity pattern are observed in both cases. In the room's air exhaust regions; it is evident that the network was able to simulate the velocity variation for the flow in the area, indicating its recognition of the pattern.

In Figure 6, 7 and 8, the relationship between temperature and velocity is also shown, but with different supply parameter values. In Figure 6, the inflow air enters the room at temperature of 15°C and a velocity of 2 m s^{-1} In Figure 7, the inflowing air enters the room at a temperature of 18ºC and a velocity of 5 m s^{-1}. In this result, a small variation in room temperature can also be observed, but the similarity in the temperature contours is evident. For the velocity in the lower part of the figure, the same similarity is seen, but with a greater difference in terms of velocity variation in the regions.

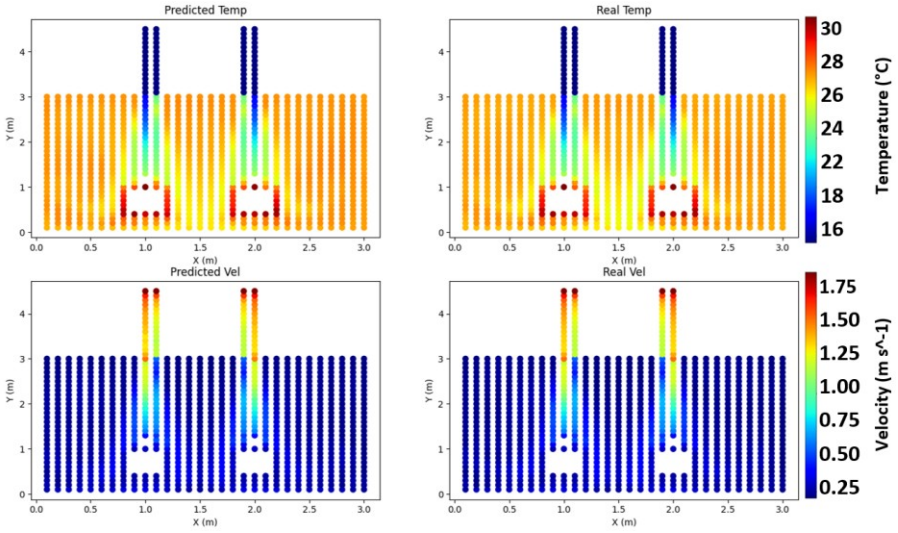

Figure 6. Middle plane room results for simulation T15V2, with temperature represented in the upper and velocity in the lower, network results on the left and CFD results on the right.

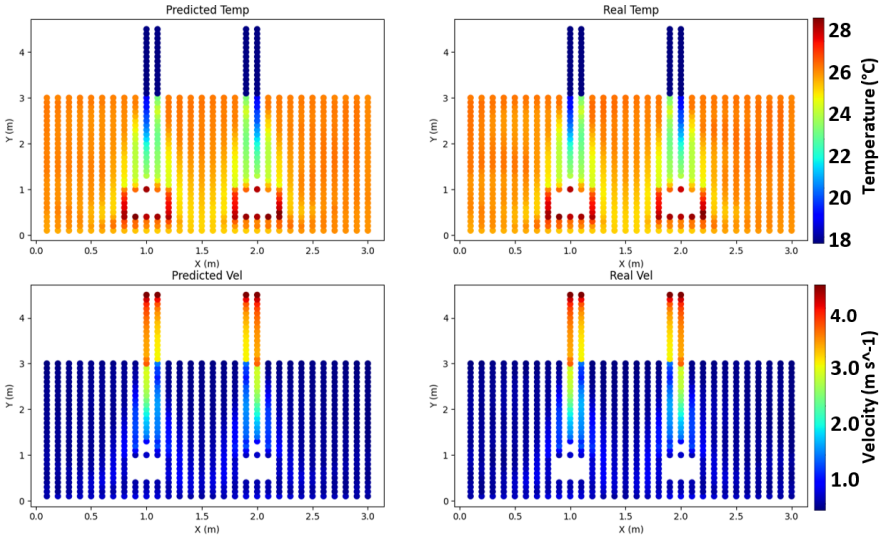

Figure 7. Middle room results for simulation T18V5, with temperature represented in the upper and velocity in the lower, network results on the left and CFD results on the right.

In Figure 8, the inflowing air enters at a temperature of 20ºC and a velocity of 3 m s^{-1}. In this case, the best result among the three was observed, with minimal variation in both temperature and velocity, both in absolute terms and in the regions with very similar contours.

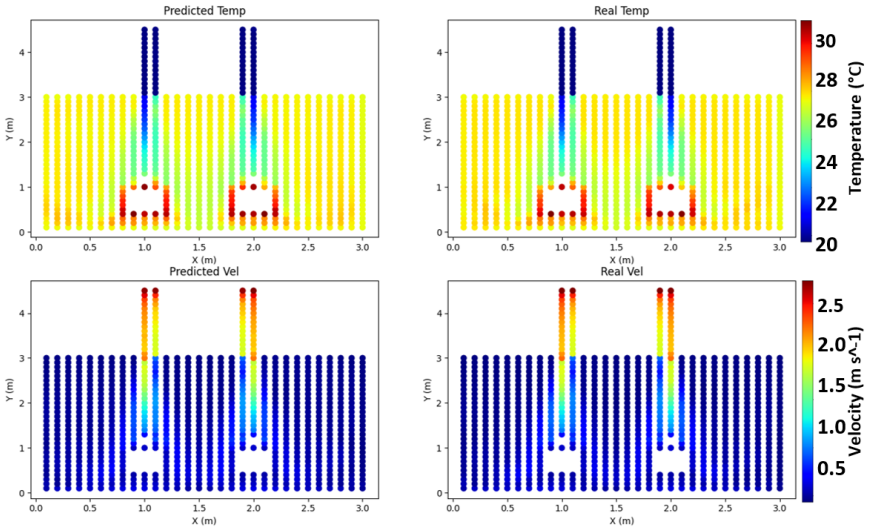

Figure 8. Middle room results for simulation T20V3, with temperature represented in the upper part and velocity in the lower part, show network results on the left and CFD results on the right.

Critical Errors

Figures 9, 10, and 11 represent the absolute error of the room for temperatures and velocities, which is the absolute difference between the network's value and the CFD simulation data. Among these results, the top 5% of the highest values were separated to potentially represent patterns of regions where the highest errors could be concentrated.

In Figure 9, the highest temperature variation is observed to be 0.4ºC, which is an acceptable value given the maximum temperature variation from 34ºC (Mannequin surface temperature) to a minimum of 18ºC (Inflow temperature) in the room. The same result had a maximum absolute velocity variation of 0.065 m s^{-1}, considering the maximum velocity variation between 0 and 2 m s^{-1}.

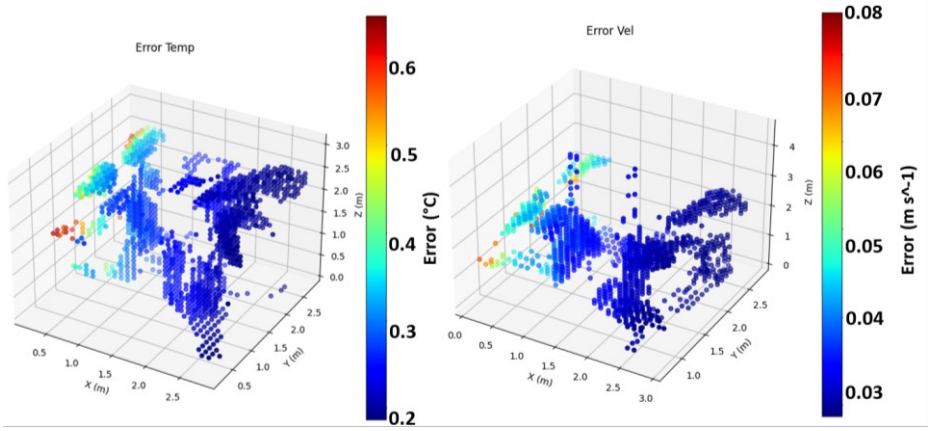

Figure 9. Critical errors for simulation T15V2.

In Figure 10, acceptable values for the maximum absolute error were also observed, being both below 0.5ºC and 0.095 m s^{-1} for temperature and velocity, respectively. In all cases, no clear error pattern was observed, indicating that the developed network does not exhibit systematic errors. It was only observed in Figure 11 that both maximum absolute errors concentrated in the same region, which is not enough to diagnose a potential pattern in the results representation.

Error distribution

A box plot of errors was generated to evaluate the percentage distribution of obtained errors. In the analysis of the box plots (Figure 12), there is a noticeable similarity between the training and test values for temperature, indicating a consistent behavior across these datasets. Conversely, in the case of velocity, the training values remained relatively low as anticipated, while the test values appeared higher but still within a margin of 0.1 m s-1. Notably, the T15V2 scenario displayed comparatively higher errors. However, despite

these disparities, the deviations remained within a 2°C difference, which aligns with the outlier range depicted in the velocity box plot. This observation suggests that although some points exhibit higher errors, they still fall within an acceptable range, warranting attention but not necessarily signaling an alarming deviation.

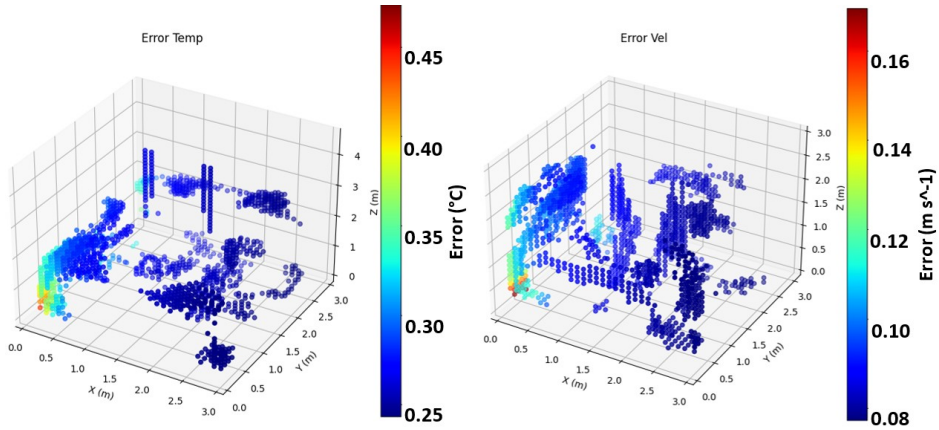

Figure 10. Criticals erros for simulation T18V5.

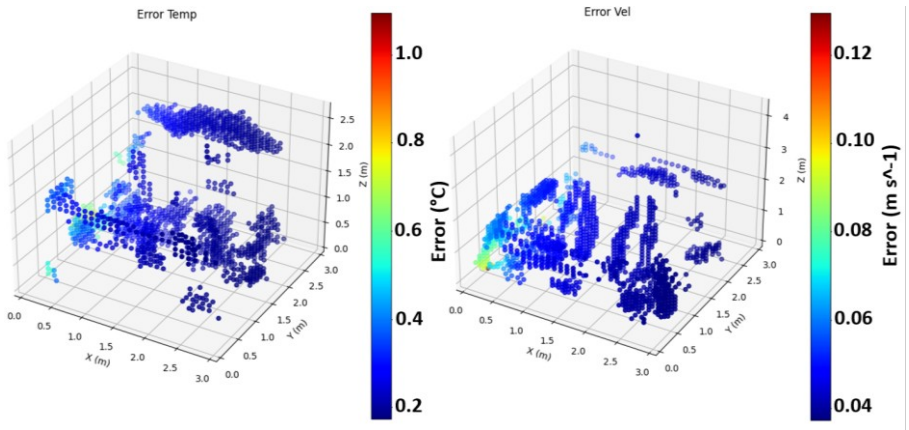

Figure 11. Critical errors for simulation T20V3.

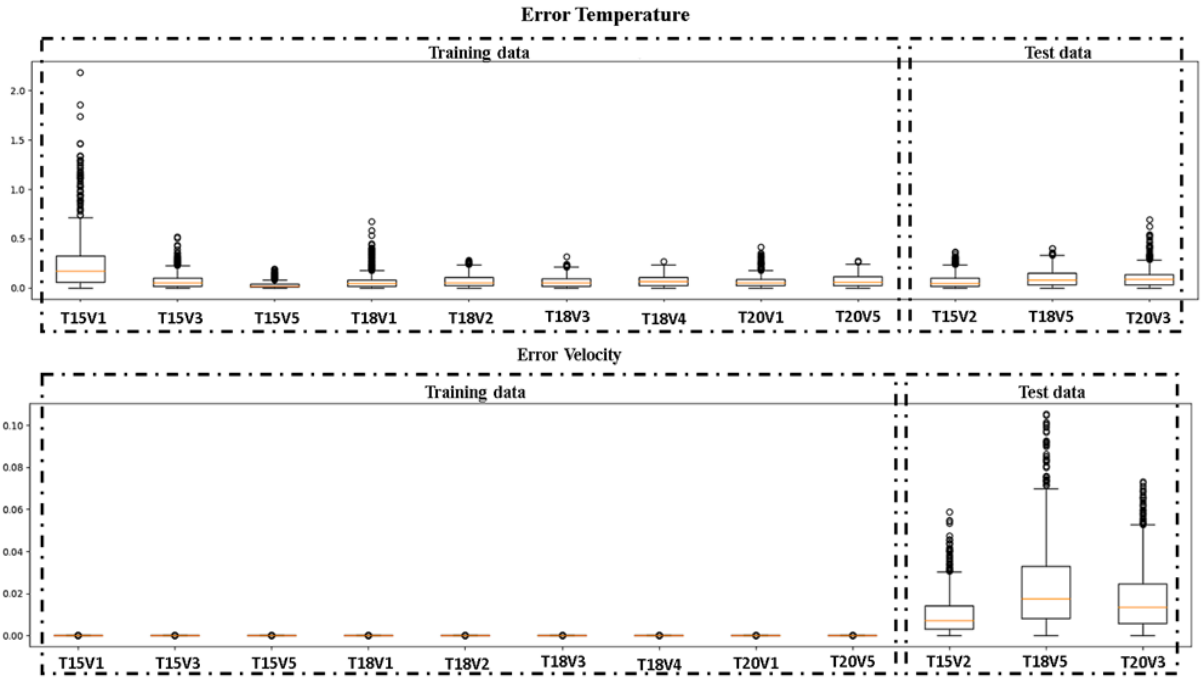

Figure 12. Box plot of errors for all simulations with the number of temperature errors represented on the top and velocity errors above.

Comparative analysis

In this study, five reference articles were selected for the purpose of comparing performance metrics as showed in Table 5. When assessing the performance of the model in comparison to these articles, it observed that the average error consistently remained below the average error presented in the article published by Zhou and Ooka (2021c). This suggests that the model demonstrates precision in predicting the variables under study. Although the maximum error exceeded that of two of the selected articles, Zhou and Ooka (2021b) and Zhou and Ooka (2021c), it is important to note that the maximum error, by itself, should not be considered the primary evaluation parameter, as it represents only an extreme point and does not reflect the overall trend of predictions.

Table 5. Comparison of results from other articles and the outcomes obtained by the network.

Metric	Zhou and Ooka (2021b)	Kim and Park (2023)	Zhou and Ooka (2021b)	Saiyad et al (2021)	Zhou and Ooka (2021c)	Results
Mean error	5%	-	-	-	-	1,87%
Maximum error	10%	-	12%	-	-	15,59%
r^2 (Temperature)	-	0,956	-	-	-	0,919
RMSE (Temperature)	-	0,237	-	0,825	0,600	0,098
r^2 (Velocity)	-	0,739	-	-	-	0,911
RMSE (Velocity)	-	0,0017	-	-	0,100	0,068

Regarding the coefficient of determination (R^2) for velocity and temperature variables, the results approached the values reported in other reference articles, demonstrating general consistency in predictions. Notably, in the velocity variable, we observed a significant difference compared to the values presented in other studies, Kim and Park (2023), indicating particularly good performance in the modeling. Furthermore, the Root Mean Square Error (RMSE) calculated for the model was considerably lower than the values obtained in the comparative articles, indicating high precision and lower dispersion in the predictions made by model.

Comprehensive room analysis

Full room results**:** In Table 6 and Table 7, the absolute errors of the test simulations for the entire room are presented. It is worth noting that these errors fall within acceptable ranges, with a maximum error of 15.59% and a maximum average error of 2.79%. The RMSE (Root Mean Square Error) for temperature and velocity remained within the maximum range of 0.107 and 0.35, respectively. This demonstrates minimal variation within the expected values commonly encountered in this context.

Table 6. Results for the temperature for full room.

	Simulation T15V2	Simulation T18V5	Simulation T20V3
Mean error	0,91%	1,86%	1,73%
Maximum error	6,38%	8,95%	9,94%
RMSE	0,082	0,106	0,107
r^2	0,971	0,924	0,864

Table 7. Results for the velocity for full room.

	Simulation T15V2	Simulation T18V5	Simulation T20V3
Mean error	1,55%	2,43%	2,79%
Maximum error	15,59%	11,62%	14,5%
RMSE	0,009	0,035	0,024
r^2	0,952	0,909	0,873

User's space results: In both Table 8 and Table 9, documenting the absolute errors of the test simulations for the entire room and the user's space, respectively, notable improvements are evident in the user's space regarding average and maximum error values compared to those of the entire room. Specifically, in the user's space, the maximum error dropped to 10.91% and the average error to 1.88%, displaying better precision. Moreover, the RMSE for temperature and velocity in both spatial areas fell within acceptable narrow ranges, emphasizing considerable improvements in error metrics, particularly in the user's space.

Table 8. Results for the temperature for user's space.

	Simulation T15V2	Simulation T18V5	Simulation T20V3
Mean error	1,04%	1,07%	1,88%
Maximum error	4,36%	5,90%	10,91%
RMSE	0,135	0,099	0,172
r^2	0,987	0,986	0,964

Table 9. Results for the velocity for user's space.

	Simulation T15V2	Simulation T18V5	Simulation T20V3
Mean error	1,76%	1,57%	1,66%
Maximum error	10,18%	8,65%	6,81%
RMSE	0,019	0,037	0,025
r^2	0,956	0,971	0,963

Jet development region: For the jet development region (Table 10 and Table 11), both maximum and average error values showed substantial improvements, with the maximum error decreasing to 7.07% and the average error to 1.05%. Furthermore, the RMSE for temperature and velocity in this specific area remained remarkably low at 0.150 and 0.035, respectively, indicating heightened accuracy in regions characterized by significant temperature gradient variations.

Table 10. Results for the temperature for jet development.

	Simulation T15V2	Simulation T18V5	Simulation T20V3
Mean error	0,57%	0,66%	1,05%
Maximum error	2,63%	3,51%	7,07%
RMSE	0,126	0,105	0,150
r^2	0,995	0,994	0,984

Table 11. Results for the velocity for jet development.

	Simulation T15V2	Simulation T18V5	Simulation T20V3
Mean error	0,62%	0,54%	0,56%
Maximum error	3,89%	3,21%	2,61%
RMSE	0,017	0,035	0,023
r^2	0,992	0,994	0,984

Conclusion

This study proposed a method for modeling the spatial distribution of temperature and velocity in Personalized Ventilation Systems (PVS) using Artificial Neural Networks (ANNs). To construct the training and improve predictions, the main pathways of network development were outlined, including data mapping and filtering, data standardization, neural network assembly, and comparative result analysis. Data were collected from CFD simulations and processed to create an input mesh for the neural networks. The ANN models were designed and trained, including hyperparameter optimization through Bayesian optimization.

The results obtained with the neural networks, as demonstrated by metrics such as RMSE, r^2, average error, and maximum error, highlight the accuracy of predictions compared to other scientific articles. Furthermore, these results were compared to reference studies, indicating that the proposed approach rivals the results of other relevant academic papers. However, it's worth noting that, as in any scientific research, some limitations and areas for improvement were identified. These include the need to consider a larger amount of simulation data for training, as well as how data treatment and mesh structure affect the results. These factors can enhance result accuracy and expand the range of values output by the network.

References

Jing, G., Ning, C., Qin, J., Ding, X., Duan, P., Liu, H., & Sang, H. (2023). Physics-guided framework of neural network for fast full-field temperature prediction of indoor environment. *Journal of Building Engineering*, *68*(1), 106054. https://doi.org/10.1016/j.jobe.2023.106054

Katramiz, E., Ghaddar, N., Ghali, K., Al-Assaad, D., & Ghani, S. (2021). Effect of individually controlled personalized ventilation on cross-contamination due to respiratory activities. *Building and Environment*, *194*, 107719. https://doi.org/10.1016/j.buildenv.2021.107719

Kim, M., & Park, H.-J. (2023). Application of artificial neural networks using sequential prediction approach in indoor airflow prediction. *Journal of Building Engineering*, *69*, 106319. https://doi.org/10.1016/j.jobe.2023.106319

Li, L., Zhang, Y., Fung, J. C. H., Qu, H., & Lau, A. K. H. (2022). A coupled computational fluid dynamics and back-propagation neural network-based particle swarm optimizer algorithm for predicting and optimizing indoor air quality. *Building and Environment*, *207*(B), 108533. https://doi.org/10.1016/j.buildenv.2021.108533

Rissetto, R., Schweiker, M., & Wagner, A. (2021). Personalized ceiling fans: Effects of air motion, air direction and personal control on thermal comfort. *Energy and Buildings*, *235*, 110721. https://doi.org/10.1016/j.enbuild.2021.110721

Saiyad, A., Patel, A., Fulpagare, Y., & Bhargav, A. (2021). Predictive modeling of thermal parameters inside the raised floor plenum data center using artificial neural networks. *Journal of Building Engineering*, *42*, 102397. https://doi.org/10.1016/j.jobe.2021.102397

Tian, X., Cheng, Y., & Lin, Z. (2022). Modelling indoor environment indicators using artificial neural network in the stratified environments. *Building and Environment*, *208*, 108581. https://doi.org/10.1016/j.buildenv.2021.108581

Xu, C., Wei, X., Liu, L., Su, L., Liu, W., Wang, Y., & Nielsen, P. V. (2020). Effects of personalized ventilation interventions on airborne infection risk and transmission between occupants. *Building and Environment*, *180*, 107008. https://doi.org/10.1016/j.buildenv.2020.107008

Xu, J., Fu, S., & Chao, C. Y. H. (2021). Performance of airflow distance from personalized ventilation on personal exposure to airborne droplets from different orientations. *Indoor and Built Environment*, *30*(10), 1643–1653. https://doi.org/10.1177/1420326X20951245

Zhou, Q., & Ooka, R. (2021a). Influence of data preprocessing on neural network performance for reproducing CFD simulations of non-isothermal indoor airflow distribution. *Energy and Buildings*, *230*, 110525. https://doi.org/10.1016/j.enbuild.2020.110525

Zhou, Q., & Ooka, R. (2021b). Neural network for indoor airflow prediction with CFD database. *Journal of Physics*, *2069*, 12154. https://doi.org/10.1088/1742-6596/2069/1/012154

Zhou, Q., & Ooka, R. (2021c). Performance of neural network for indoor airflow prediction: Sensitivity towards weight initialization. *Energy and Buildings*, *246*, 111106. https://doi.org/10.1016/j.enbuild.2021.111106